Measurements and Path Loss Models at 30 and 300 MHz over Flat Terrain Scenarios

Nektarios Moraitis(1), Panayiotis Frangos(1), Ileana Popescu(1), Alexandros Rogaris(1) and Seil Sautbekov(2)

(1)School of Electrical and Computing Engineering, National Technical University of Athens (NTUA),
9, Iroon Polytechniou Str., 157 73 Zografou, Athens, Greece
Tel. : +30 210 772 3694;   e-mail : pfrangos@central.ntua.gr

(2)Department of Physics and Technology, Al-Farabi Kazakh National University
Almaty, Kazakshtan
e-mail : sautbek@mail.ru

Abstract

In this paper an outdoor measurement campaign for almost flat terrain environment is undertaken for wireless mobile applications at the frequencies of 30 MHz and 300 MHz. The measured results are compared here both with the well – known in the literature "Two–Ray" (TR) model of wave propagation, as well as with the also well – known "Extended Hata" (EH) and "Egli" empirical models. The results showed that TR model forecasts path loss with better accuracy, delivering low error metrics. It outperforms Extended Hata and Egli models, which proved to be unsuitable for predicting path loss in the specific examined scenario.

It is intended that further research by our research group will be conducted in the direction of comparison of our measured results with alternative analytical results, which have been produced by us in previous publications of ours, in this "low frequency" regime.

1. Introduction

The problem of electromagnetic (EM) wave propagation over a flat terrain (or over a lossy medium with flat interface) is well – known in the literature as the *"Sommerfeld antenna radiation problem"*, where the interest here is for observation points over the flat interface [1-23]. However, in this paper we concentrate in comparing our outdoor experimental measurements in "low frequency" regime (here for frequencies 30 MHz and 300 MHz), which are obtained here by our research group, with approximate or empirical models of electromagnetic (EM) wave propagation [24-30]. In near future proposed research by our group, we intend to compare our outdoor experimental results measured by us here with alternative analytical results which have been produced by our research group in previous publications of ours (also in the "low frequency" regime, at which *surface waves* are expected to be present).

The rest of this paper is organized as follows : Section 2 describes the measurement environment, the equipment, as well as the procedure followed during our outdoor experimental campaign. In Section 3, different models are introduced and assessed for their suitability to forecast the measured path loss. Finally, interesting conclusions and future research are presented in Section 4.

2. Experimental campaign

The measurements were carried out in a flat road inside our University (NTUA) campus, in order to represent a near flat earth scenario. Fig. 1(a) and Fig. 1(b), illustrate the measurement environment, as well as the location of the transmitter (Tx). The *blue line* indicates the trajectory of the receiver (Rx) at 30 MHz, along which, the electric field values were recorded from 2 m up to 100 m in steps of 2 m. In respect, the *red line* stands for the 300 MHz measurements, where the electric field values were recorded from 2 m up to 300 m in steps of 2 m. Both sides of the road were surrounded by tall trees. The *yellow star* denotes the location of the Tx, which transmitted a continuous wave (CW) signal at 30 MHz and 300 MHz, for the first and second low frequency regime scenarios, respectively. In total, 50 and 150 received signal power samples were recorded at 30 and 300 MHz, respectively. At each measurement position the Rx was stationary, having a line-of-sight (LOS) condition with the Tx .

The Tx antenna was mounted at a height of 3 m about the road surface. A signal generator was employed to produce the transmitted signal, which was fed, through a 3-m cable, to a *vertically polarized* omnidirectional antenna (Skycan 25-2000 MHz), with a half power beamwidth (HPBW) of 60° in the elevation plane and a constant gain of about -25 dBi and 0 dBi, in the azimuth plane, at 30 MHz and 300 MHz, respectively. The transmitted effective isotropic radiated power (e.i.r.p.), was 20 dBm at both selected frequencies.

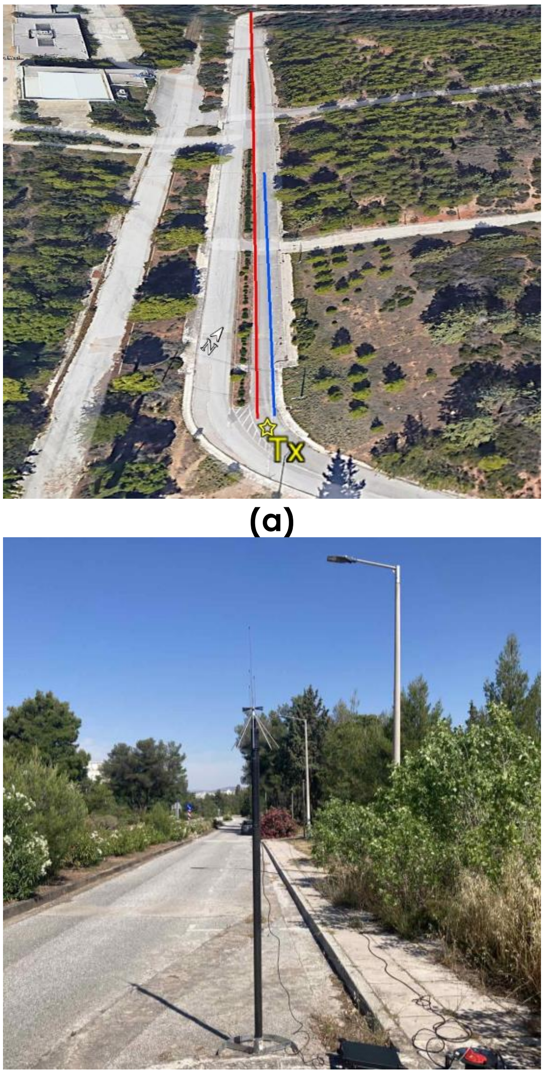

(a)

(b)

Figure 1. Measurement environment.

An SRM-3006 frequency selective field meter by Narda GmbH (Pfullingen, Germany) in spectrum analysis mode was employed as the receiving unit. An electric field isotropic probe was used (27 MHz - 3 GHz with a 0 dBi gain), connected to the main control unit through a 1.5-m cable. The Rx sensor was mounted on a wooden tripod at 1.7 m above the field surface. The Rx unit recorded the power samples in dBV/m, using a time average of 2 minutes. The utilized Rx equipment was calibrated according to the ISO/IEC 17025:2017 standard [24]. Table I summarizes the Tx and Rx characteristics adopted in the launched measurement campaign.

TABLE I. Transmitter and receiver characteristics during the measurement campaign at each selected frequency scenario

	30 MHz	300 MHz
Tx power	20 dBm	20 dBm
Tx gain	0 dBi	-25 dBi
EIRP	20 dBm	-5 dBm
Rx gain	0 dBi	
Rx sensitivity	-65 dBm	

Based on the received signal power the measured path loss PL, in decibels, at each Rx location can be calculated by:

$$PL = \mathrm{P}_{\mathrm{Tx}} + G_{\mathrm{Tx}} + G_{\mathrm{Rx}} - P_r \qquad (1)$$

where P_{Tx} indicates the Tx power in dBm, G_{Tx}, G_{Rx} denotes the Tx and Rx gains, respectively, in dBi, and P_r stands for the received signal power in dBm. Therefore, from (1), 50 and 150 path loss samples are resolved at each examined frequency scenario at a specific distance d_D, in meters, between Tx and Rx (length of the direct ray) that is given by:

$$d_D = \sqrt{d^2 + (h_t - h_r)^2} \qquad (2)$$

where d designates the direct horizontal (ground) distance, in meters, between Tx and Rx, and h_t, h_r designate the Tx and Rx heights (3 and 1.7 m), respectively.

The raw data for both scenarios are shown in Fig. 2, where the received power versus distance is depicted. It should be pointed out that the distance from Tx, in meters, represents the direct distance (d_D) between Tx and Rx.

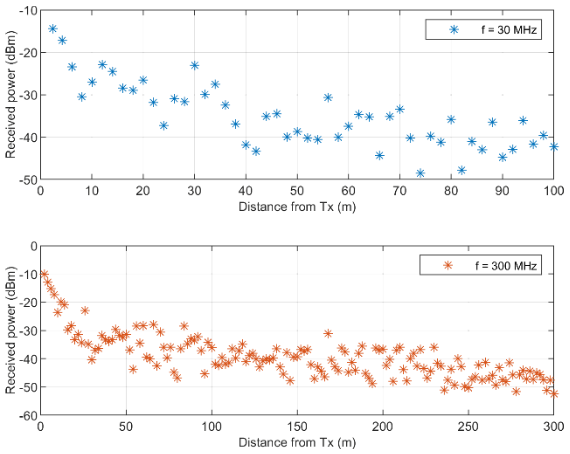

Figure 2. Received signal power at each measured scenario at 30 and 300 MHz.

In Section 3, below, the measured path loss, from eq. (1) above, will be compared with the flat terrain model ('two – ray model'), as well as with two empirical models for comparison purposes, which are the 'Extended Hata model' and 'Egli model'.

3. Path loss models, results and discussion

The '*two-ray model*' describes the signal propagation using two components. The direct ray between Tx and Rx and a ground reflected path ray. The path loss, in decibels, based on the two-ray model is given by [25]:

$$PL = 20\log_{10}\left(\frac{4\pi d}{\lambda}\right) - 20\log_{10}\left|1+\Gamma_V\, e^{j\Delta\varphi}\right| \quad (3)$$

where λ is the wavelength, in meters, at each selected frequency, and d is the ground (horizontal) distance between Tx and Rx, as previously mentioned. Furthermore, Γ_V denotes the vertical polarization reflection coefficient of the ground reflected path, and $\Delta\varphi$ stands for the phase difference between the direct and the ground paths. The reflection coefficient is described by:

$$\Gamma_V = \frac{-\varepsilon_r \sin\theta_i + \sqrt{\varepsilon_r - (\cos\theta_i)^2}}{\varepsilon_r \sin\theta_i + \sqrt{\varepsilon_r - (\cos\theta_i)^2}} \quad (4)$$

where θ_i, is the *"grazing angle"* of the incident wave (i.e., the angle between the incident EM wave and the flat terrain), and ε_r is the relative permittivity of the ground. Assuming a very dry ground, ε_r = 3 according to [26]. Furthermore, the grazing angle in (4), is related to the geometrical propagation characteristics according to:

$$\sin\theta_i = \left(\frac{h_t + h_r}{d_G}\right) \qquad \cos\theta_i = \left(\frac{d}{d_G}\right) \quad (5)$$

where d_G denotes the length of the ground reflected ray, in meters, which can be calculated by:

$$d_G = \sqrt{d^2 + (h_t + h_r)^2} \quad (6)$$

Finally, the phase difference between of the path lengths between the direct and the ground reflected rays are given by:

$$\Delta\varphi = \frac{2\pi}{\lambda}(d_D - d_G) \quad (7)$$

where d_D and d_G are provided by (2) and (6), respectively.

Apart from the two-ray path loss model, the measured path loss is also compared with the *"Extended Hata"* model [27]. The specific model is widely used and is applicable for frequencies up to 3 GHz, and distances up to 40 km. A rural/open area environment is assumed in this case; therefore, the path loss is given by:

$$PL = PL_U - 4.78(\log_{10}[\min\{\max\{150, f\},2000\}])^2 + 18.33\log_{10}[\min\{\max\{150, f\},2000\}] - 40.94 \quad (8)$$

where f is the operating frequency in MHz, and PL_U the path loss considering the urban environment. The latter parameter for frequencies between below 150 MHz can be calculated according to:

$$PL_U = 69.6 + 26.2\log_{10}(150) - 20\log_{10}(150/f) - 13.82\log_{10}(\max\{30, h_t\}) + (44.9 - 6.55\log_{10}(\max\{30, h_t\}))\log_{10}(d_D) - a(h_r) - b(h_t) \quad (9)$$

where d_D is the direct ray distance, converted in kilometres, between Tx and Rx, and f the operating frequency in MHz. Further, $a(h_r)$ and $b(h_t)$, are the correction factors for the Rx and Tx, respectively, taking into account their specific heights h_r and h_t in meters. The correction factors are adopted for the rural/open area locations and can be calculated by :

$$b(h_t) = \min\{0, 20\log_{10}(h_t / 30)\} \quad (10)$$

and

$$a(h_r) = (1.1\log_{10}(f) - 0.7)\min\{10, h_r\} - (1.56\log_{10}(f) - 0.8) + \max\{0, 20\log_{10}(h_r/10)\} \quad (11)$$

For frequencies between 150 and 1500 MHz, the path loss is expressed as:

$$PL_U = 69.6 + 26.2\log_{10}(f) - 13.82\log_{10}(\max\{30, h_t\}) + (44.9 - 6.55\log_{10}(\max\{30, h_t\}))\log_{10}(d_D) - a(h_r) - b(h_t) \quad (12)$$

Therefore, the *"Extended Hata"* model calculates differently the path loss at 30 and 300 MHz, leveraging (9) and (12), espectively. Finally, *"Egli"* model [28], is also popular and utilized in forecasting path loss over terrain scenarios. It is applicable for low frequencies between 40 and 1000 MHz and for distances up to 10 km. The path loss is given, in decibels, according to

$$PL_{Egli} = 91.2 + 40\log_{10}(d_D) - 20\log_{10}(h_t h_r) + 20\log_{10}(f) \quad (13)$$

where d_D stands for the direct distance, converted in kilometres, between Tx and Rx, f designates the operating frequency in MHz, and h_t, h_{tr}, denote the Tx and Rx heights, respectively.

The results are presented in Fig. 3 where the path loss versus distance (in logarithmic scale) is provided along with the three different models for comparison.

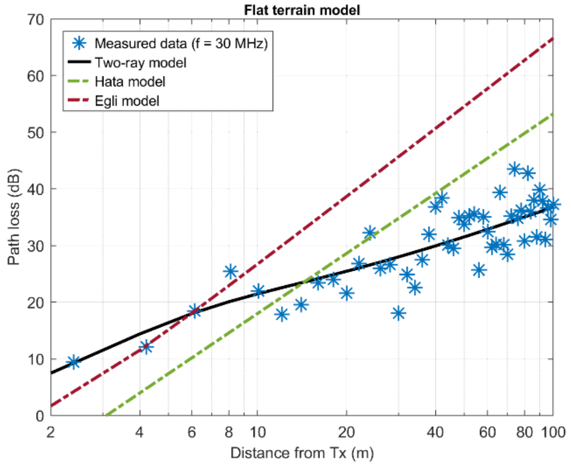

(a)

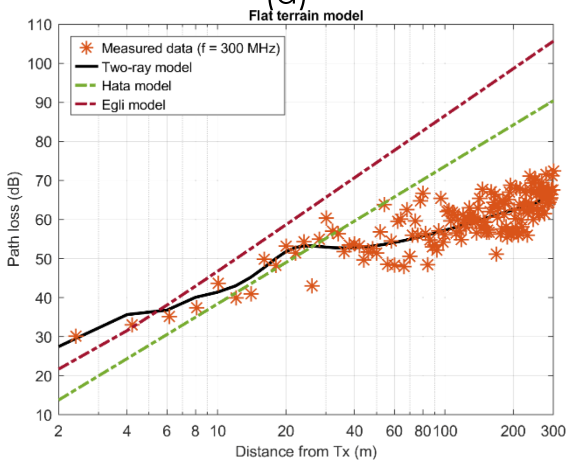

(b)

Figure 3. Path loss results versus distance. (a) 30 MHz and (b) 300 MHz.

The results reveal that the "two-ray model" fits better to the measured samples. This can be credited to the geometrical nature of the applied model that considers the physical characteristics of the propagating signal over the flat terrain environment. This behaviour is apparent in both examined frequencies according to Fig. 3, although at 30 MHz the shadow fading (i.e., the path loss variations with respect to the two-ray model) are greater at 30 MHz, probably due to reflections from surrounding objects. Lower shadow fading is observed at 300 MHz.

Furthermore, both the "Extended Hata" and "Egli" models do not adapt well to the measured data at both 30 and 300 MHz. This is probably due to the low Tx and Rx heights that were used during the measurement campaign, which limits these two models' applicability. It is also worth commenting that both the "Extended Hata" and "Egli" models predict well the path loss in the first few meters at both examined frequencies (about 10 m for 30 MHz and 30 m at 300 MHz). However, after these distances, large discrepancies are encountered, between the measured and the predicted path loss.

In order to validate and compare quantitively the prediction accuracy, specific statistical metrics are applied, thereby determining the error between the measured and the forecasted path loss [29], [30], [31], [32]. The mean absolute error (MAE), in decibels, is given by :

$$\mathrm{MAE} = \frac{1}{N}\sum_{i=1}^{N}\left|PL_i^{meas} - PL_i^{pred}\right| \quad (14)$$

where PL_i^{meas} and PL_i^{pred} stand for the measured and predicted path loss values, respectively, and *i* is the index of the measured sample. Finally, *N* is the total number of path loss samples. The mean absolute percentage error (MAPE) is calculated according to:

$$\mathrm{MAPE} = \frac{1}{N}\sum_{i=1}^{N}\left|\frac{PL_i^{meas} - PL_i^{pred}}{PL_i^{meas}}\right| \times 100\% \quad (15)$$

Further, the root mean square error (RMSE), which actually represents the shadow factor is given, in decibels, by:

$$\mathrm{RMSE} = \sqrt{\frac{1}{N}\sum_{i=1}^{N}\left(PL_i^{meas} - PL_i^{pred}\right)^2} \quad (16)$$

Finally, the cross-correlation coefficient reveals the degree of relationship between the measured and predicted samples. It is defined as the Pearson product moment [33], and can be calculated according to:

$$\rho = \frac{\sum_{i=1}^{N}\left(PL_i^{meas} - \overline{PL_i^{meas}}\right)\left(PL_i^{pred} - \overline{PL_i^{pred}}\right)}{\sqrt{\sum_{i=1}^{N}\left(PL_i^{meas} - \overline{PL_i^{meas}}\right)^2 \sum_{i=1}^{N}\left(PL_i^{pred} - \overline{PL_i^{pred}}\right)^2}} \quad (17)$$

Cross-correlation is a nonparametric measure of the statistical dependence among the measured and the forecasted path loss. Based on the absolute value the coefficient, the correlation between the measurements and the prediction can be classified as strong for values 0.6-0.79 and very strong for values 0.8-1.0 [31]. Acceptable correlation values are those greater than 0.8 that validate the appropriateness of an assessed model [34].

The statistical errors are determined in the following, by using (14)-(17), for each examined model. Table II summarizes the numerical results for each evaluated model and frequency scenario.

TABLE II. Statistical results between measured and predicted path loss for Two-Ray (TR), Extended Hata (EH) and Egli (EG) models at each frequency scenario

Model	Metric	30 MHz	300 MHz
TR	MAE [dB]	**3.3**	**3.2**
	MAPE [%]	**1.9**	**1.5**
	RMSE [dB]	**4.3**	**4.0**
	ρ	**0.84**	**0.85**
EH	MAE [dB]	**10.7**	**9.4**
	MAPE [%]	**9.5**	**8.2**
	RMSE [dB]	**12.0**	**11.1**
	ρ	**0.76**	**0.79**
EG	MAE [dB]	**13.7**	**13.1**
	MAPE [%]	**11.4**	**10.2**
	RMSE	**15.6**	**14.7**

	[dB]		
	ρ	**0.61**	**0.66**

The results in Table II reveal that "Two-Ray" (TR) model is better applicable in a near flat-terrain environment, that is much lower errors are obtained, as compared with the "Extended Hata" (EH) and "Egli" (EG) models. In terms of RMSE, TR model fits better at 300 MHz, although the errors between (for TR model) 30 and 300 MHz can be regarded as comparable.

On the other hand, EH and EG models exhibit much higher errors, with EG model to be inferior between all the examined models. Despite the high errors, EH and EG models seem to adapt better at 300 MHz, which indicates that are more appropriate at higher frequency applications over near flat terrain scenarios. However, disappointing results are encountered at 30 MHz, where very high errors and very low correlations are obtained. Finally, it is proved that empirical models, such as EH and EG are not recommended for near flat-terrain and low frequency scenarios providing inaccurate forecasts.

4. Conclusion

In this paper we presented an outdoor experimental measurement campaign of our research group from propagation of EM waves over flat terrain at 30 MHz and 300 MHz ('low frequencies' in our 'language', where 'surface waves' may exist). The measured data were compared with Extended Hata and Egli empirical models, as well as with the two-ray geometrical optic model. According to the statistical analysis it is observed that the latter model exhibits the best performance predicting the path loss with remarkable accuracy in both examined frequency scenarios.

As possible future work, the authors would like to assess additional path loss models of theirs (obtained by them previously through their previous analytical EM propagation methods above flat terrain), and validate their suitability to predict accurately the path loss in near flat-terrain scenarios.

Acknowledgement

The authors would like to thank the Ministry of Education and Science of the Republic of Kazakhstan (Grant No. AP19676900), which supported this research. In addition, they would like to thank Ph.D. candidate Mr. Basil Massinas (at NTUA) for his valuable help in the preparation of this paper.

References

[1] A. N. Sommerfeld, "Propagation of waves in wireless telegraphy," *Ann. Phys.*, 1909, 28, pp. 665-737.

[2] K. A. Norton, "The propagation of radio waves over the surface of the earth and in the upper atmosphere," *Proc. Inst. Radio Eng.*, vol. 24, no. 10, pp. 1367-1387, Oct. 1935. doi:10.1109/JRPROC.1936.227360.

[3] A. K. Norton, "The propagation of radio waves over the surface of the earth and in the upper atmosphere," *Proc. Inst. Radio Eng.*, vol. 25, no. 9, pp. 1203-1236, Sep. 1937. doi:10.1109/JRPROC.1937.228544.

[4] J. Wait, "Launching a surface wave over the earth," *Electron. Lett.*, vol. 3, no. 9, pp. 396-397, Sep. 1967. doi:10.1049/el:19670307.

[5] R. J. King, "Electromagnetic wave propagation over a constant impedance plane," *Radio Sci.* 1969, 4, pp. 255-268, doi:10.1029/RS004i003p00255.

[6] T. K. Sarkar, W. Dyab, M. N. Abdallah, M. Salazar-Palma, M. V. S. N. Prasad, S. W. Ting, and S. Barbin, "Electromagnetic macro modeling of propagation in mobile wireless communication: Theory and experiment," *IEEE Antennas Propag. Mag.*, 2012, 54, pp. 17-43, doi:10.1109/MAP.2012.6387779.

[7] J.G.V. Bladel, *The Sommerfeld Dipole Problem. In Electromagnetic Fields*, J. Wiley and Sons, Inc.: Hoboken, NJ, USA, 2007; Section 9.3, pp. 448–452.

[8] G. Tyras, *Field of a Dipole in a Stratified Medium. In Radiation and Propagation of Electromagnetic Waves*; Academic Press, Inc., New York, NY, USA, 1969; Section 6, pp. 133–160.

[9] Y. Rahmat-Samii, R. Mittra, P. Parhami, "Evaluation of Sommerfeld Integrals for Lossy Half-Space Problems". *Electromagnetics,* 1981, 1, pp. 1–28, doi:10.1080/02726348108915122.

[10] R. E. Collin, "Hertzian dipole radiating over a lossy earth or sea: some early and late 20th-century controversies". *IEEE Antennas Propag. Mag.,* 2004, 46, pp. 64–79, doi:10.1109/MAP.2004.1305535.

[11] K. A. Michalski, "On the efficient evaluation of integral arising in the sommerfeld halfspace problem". *IEE Proc.-Microwaves, Antennas Propag.,* 1985, 132, pp. 312–318, doi:10.1049/ip-h-2.1985.0056.

[12] G. Pelosi, J. L. Volakis, "On the Centennial of Sommerfeld's Solution to the Problem of Dipole Radiation Over an Imperfectly Conducting Half Space", *IEEE Antennas Propag. Mag.,* 2010, 52, pp. 198–201, doi:10.1109/MAP.2010.5586629.

[13] J. R. Wait, "The Ancient and Modern History of EM Ground-Wave Propagation.", *IEEE Antennas Propag. Mag.,* 1998, 40, pp. 7–24, doi:10.1109/74.735961.

[14] A. Baños, *Dipole Radiation in the Presence of a Conducting Half-Space*, Pergamon Press, Oxford, UK, 1966; pp. 151–158.

[15] S.S. Sautbekov, R.N. Kasimkhanova,; P.V. Frangos, *"Modified Solution of Sommerfelds's Problem:*, In Proceedings of the CEMA'10 Conference, Athens, Greece, 7–9 October 2010; pp. 5–8. Available online: http://rcvt.tu-sofia.bg/CEMA/proceedings/CEMA_2010_proc.pdf (accessed on May 2021).

[16] S. Sautbekov, "The Generalized Solutions of a System of Maxwell's Equations for the Uniaxial Anisotropic Media. In Electromagnetic Waves Propagation in Complex Matter"; *IntechOpen Limited*: London, UK, 2011; Chapter 1, pp. 1–24, doi:10.5772/16886.

[17] K. Ioannidi, C. Christakis, S. Sautbekov, P. Frangos, and S. K. Atanov, "The Radiation Problem from a Vertical Hertzian Dipole Antenna above Flat and Lossy Ground: Novel Formulation in the Spectral Domain with Closed–Form Analytical Solution in the High Frequency Regime," *Int. J. Antennas Propag. (IJAP)*, 2014, Special Issue on 'Propagation of Electromagnetic Waves in Terrestrial Environment for Applications in Wireless Telecommunications', doi:10.1155/2014/989348.

[18] S. Bourgiotis, K. Ioannidi, C. Christakis, S. Sautbekov, P. Frangos, "The Radiation Problem from a Vertical Short Dipole Antenna Above Flat and Lossy Ground: Novel Formulation in the Spectral Domain with Numerical Solution and Closed-Form Analytical Solution in the High Frequency Regime", *Proceedings of CEMA'14 Conference*, Sofia, Bulgaria, 16–18 October 2014; pp. 12–18, Available online: http://rcvt.tu-sofia.bg/CEMA/proceedings/CEMA_2014_proc.pdf (accessed on May 2021).

[19] S. Bourgiotis, A. Chrysostomou, K. Ioannidi; S. Sautbekov and P. Frangos, "Radiation of a Vertical Dipole over Flat and Lossy Ground using the Spectral Domain Approach: Comparison of Stationary Phase Method Analytical Solution with Numerical Integration Results", *Electronics and Electrical Engineering Journal,* 2015, 21, pp. 38–41, doi:10.5755/j01.eee.21.3.10268.

[20] A. Chrysostomou, S. Bourgiotis, S. Sautbekov, K. Ioannidi, and P. Frangos, "Radiation of a Vertical Dipole Antenna over Flat and Lossy Ground: Accurate Electromagnetic Field Calculation using the Spectral Domain Approach along with Redefined Integral Representations and corresponding Novel Analytical Solution," *Electronics and Electrical Engineering Journal,* 2016, 22, pp. 54–61, doi:10.5755/j01.eie.22.2.14592.

[21] S. Sautbekov, S. Bourgiotis, A. Chrysostomou, and P. Frangos, "A Novel Asymptotic Solution to the Sommerfeld Radiation Problem: Analytic Field Expressions and the Emergence of the Surface Waves," *PIER M*, 2018, 64, pp. 9–22, doi:10.2528/PIERM17082806.

[22] S. Bourgiotis, P. Frangos, S. Sautbekov and M. Pshikov, "The Evaluation of an Asymptotic Solution to the Sommerfeld Radiation Problem using an Efficient Method for the Calculation of Sommerfeld Integrals in the Spectral Domain", *'Electronics' Journal*, MDPI Publisher, 1, https://doi.org/10.3390/electronics1010000, https://www.mdpi.com/journal/electronics, Special Issue on 'Propagation of Electromagnetic Waves in Terrestrial Environment for Applications in Wireless Telecommunications and Radar Systems', June 2021.

[23] J. Fikioris, *Introduction to Antenna Theory and Propagation of Electromagnetic Waves;* National Technical University of Athens: Athens, Greece, 1982. (In Greek).

[24] International Organization for Standardization, "General requirements for the competence of testing and calibration laboratories," ISO/IEC 17025:2017, Geneva, Switzerland, Nov. 2017.

[25] T. S. Rappaport, *Wireless Communications: Principles and Practice*. (2nd ed.), Prentice Hall, Upper Saddle River, New Jersey, 2002.

[26] Electrical Characteristics of the Surface of the Earth, document ITU-R P.527-6, International Telecommunication Union, Geneva, Switzerland, Sep. 2021.

[27] Monte Carlo simulation methodology for the use in sharing and compatibility studies

between different radio services or systems, document ITU-R SM.2028-2, International Telecommunication Union, Geneva, Switzerland, Jun. 2017.

[28] J. J. Egli, "Radio Propagation above 40 MC over irregular terrain," Proc. IRE, vol. 45, no. 10, pp. 1383-1391, Oct. 1957.

[29] E. Östlin, H. J. Zepernick, and H. Suzuki, "Macrocell path-loss prediction using artificial neural networks," *IEEE Trans. Veh. Technol.*, vol. 59, no. 6, pp. 2735-2747, Jul. 2010.

[30] Y. Zhang, *et al.*, "Path loss prediction based on machine learning: Principle, method, and data expansion," *Appl. Sci.*, vol. 9, no. 9, pp. 1-18, May 2019.

[31] J. D. Parsons, *The Mobile Radio Propagation Channel.* 2nd ed., New York: Wiley, 2000.

[32] X. Zhou, *et al.*, "Experimental characterization and correlation analysis of indoor channels at 15 GHz," *Int. J. Antennas Propag.*, Article ID 601835, 2015.

[33] W. C. Y. Lee, *Mobile communications design fundamentals*. Wiley series in telecommunications and signal processing. Wiley, 1993.

[34] M. J. Campbell and & T. D. V. Swinscow. *Statistics at Square One*. (11th ed.). Wiley, 2011.